THE JOURNAL OF PHYSICAL CHEMISTRY A

Article

Cite This: J. Phys. Chem. A 2018, 122, 700−707

pubs.acs.org/JPCA

Theoretical Study of pK_a Values for Trivalent Rare-Earth Metal Cations in Aqueous Solution

Donghai Yu,[†,§] Ruobing Du,[†] Ji-Chang Xiao,*[,†] Shengming Xu,*[,‡] Chunying Rong,[†] and Shubin Liu*[,∥]

[†]Key Laboratory of Organofluorine Chemistry, Shanghai Institute of Organic Chemistry, University of Chinese Academy of Sciences, Chinese Academy of Sciences, 345 Lingling Road, Shanghai 200032, China

[‡]Institute of Nuclear and New Energy Technology, Tsinghua University, Beijing 100084, China

[§]Key Laboratory of Chemical Biology and Traditional Chinese Medicine Research (Ministry of Education of China), College of Chemistry and Chemical Engineering, Hunan Normal University, Changsha, Hunan 410081, China

[∥]Research Computing Center, University of North Carolina, Chapel Hill, North Carolina 27599-3420, United States

Supporting Information

ABSTRACT: Molecular acidity of trivalent rare-earth metal cations in aqueous solution is an important factor dedicated to the efficiency of their extraction and separation processes. In this work, the aqueous acidity of these metal ions has been quantitatively investigated using a few theoretical approaches. Our computational results expressed in terms of pK_a values agree well with the tetrad effect of trivalent rare-earth ions extensively reported in the extraction and separation of these elements. Strong linear relationships have been observed between the acidity and quantum electronic descriptors such as the molecular electrostatic potential on the acidic nucleus and the sum of the valence natural atomic orbitals energies of the dissociating proton. Making use of the predicted pK_a values, we have also predicted the major ionic forms of these species in the aqueous environment with different pH values, which can be employed to rationalize the behavior difference of different rare-earth metal cations during the extraction process. Our present results should provide needed insights not only for the qualitatively understanding about the extraction and separation between yttrium and lanthanide elements but also for the prediction of novel and more efficient rare-earth metal extractants in the future.

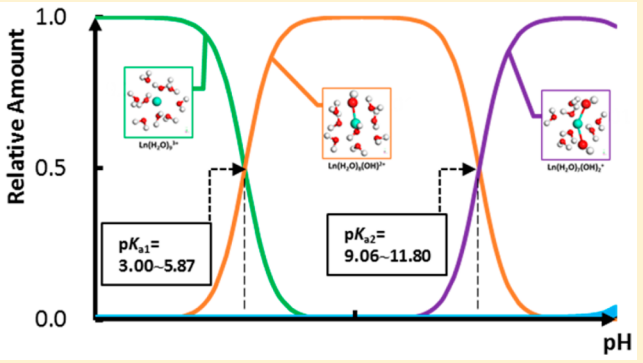

1. INTRODUCTION

The pK_a value of a molecular system is defined as the negative logarithm of its acidic equilibrium dissociation constant. It is a fundamental physical chemistry property and widely used to measure the acidity of a substance quantitatively.[1−4] It is a critical parameter in drug design,[5] biological metabolism,[6,7] chemical synthesis, environmental protection, toxicology, and industrial catalysis. An aqueous metal ion exists in a hydrated form, i.e., as a metal−water complex, and in practice, its acidity is the acidity of the water molecule coordinated to the metal center.[8,9] Aqueous metal pK_a values are important because of the global distribution of metal ions in water, which significantly influence metal gathering, separation,[10] catalytic properties, and toxicity.[11] Metal pK_a values can be determined by using various techniques such as ultraviolet−visible, infrared, Raman, nuclear magnetic resonance spectroscopies, specific conductance, and electromotive force measurements.[12] For example, a series of referential metal pK_a values were determined using an electromotive force method by Sillén.[12] A spectroscopic method and a simple hydrolysis model were developed by Jordan and co-workers[8] to determine the first-order hydrolysis equilibrium constants of Co(III) and Mn(III). The concentrations of several possible forms of Co(III) and Mn(III) were determined, and their results showed that $[Mn(H_2O)_6]^{3+}$ had the highest acidity because of its Jahn−Teller distortion and coordinating properties.[13] One of the difficulties in determining aqueous metal pK_a values is that ionic forms are indistinguishable. Even the most advanced techniques such as extended X-ray absorption fine structure spectroscopy and large-angle X-ray scattering,[14−16] which are used to identify the coordination conditions, cannot distinguish directly between OH^- or H_2O coordinated to a metal center because hydrogen is invisible, so the definite ratio of different forms cannot be accurately determined. Consequently, there are many difficulties associated with obtaining accurate aqueous metal pK_a values using experimental approaches such as direct measurement of the molecular

Received: December 7, 2017
Published: December 20, 2017

DOI: 10.1021/acs.jpca.7b12074
J. Phys. Chem. A 2018, 122, 700−707

acidity using titrimetry.[17] Because of these, reported pK_{a1} values of La(III) change dramatically in the literature, ranging from 5.6 to 10.1.[18]

An alternative way to obtain pK_a values for metal ions is from the computational study.[19] Using an experiential arithmetic Fortran-based program was first reported in the 1960s.[20] Later, metal acidities or pK_a values were calculated more accurately based on the thermodynamics energies of the corresponding hydrolysis reactions using ab initio, density functional theory (DFT), and other quantum chemical methods.[8,9,14,21,22] Appropriate uses of reliable and robust models and protocols could give rise to computational results that can be as accurate as experiment data. These processes could provide in-depth and intuitive understanding about possible intermediate forms, which are not available for experimental means.[14,23,24] For instance, acidities and hydrolysis properties of nine trivalent ions were evaluated quantitatively from proton-binding energies of their hydroxides by Rustad.[25] A combined DFT calculation with experimental measurements proposed a good linear relationship between the energy and metal pK_a.[11−13] In addition, the aqueous metal acidity was investigated by the gaseous computation of hydrolysis reaction, as Stace reported.[8] Their results showed that the pK_a value is correlated with the number of coordinated water molecules, which decreases with the increasing number of water molecules. Moreover, several factors that affect the precision of pK_a calculations, such as the coordination model, choice of density functionals, and solvation effects,[26] were studied by Sweeney and Rustad.[14] They reported that pK_a values obtained from a hydrolysis model can be used to accurately measure the acidity of metal ions.[23,25] At the same time, one of the present authors and his co-workers performed a theoretical study on metal pK_a values on the basis of DFRT (density functional reactivity theory). Their results suggest that the rule of computing the pK_a value of a hydrated ion is similar to that of common organic acids, and that its acidity can be simulated by molecular energy changes caused by proton dissociation,[22,27] resulting in linear correlations between pK_a values and the molecular electrostatic potential (MEP) or the sum of the valence natural atomic orbitals energies (NAO) on the dissociating proton and acidic atom.[3,4,22,28−30]

Rare-earth metals, called industrial vitamins,[31] are important and widely used in catalysis, electromagnetism, optics, agriculture, and advanced materials. The pK_a value of aqueous rare-earth metals directly or indirectly influences their applications in these fields. In particular, rare-earth metal pK_a values significantly affect their extraction, separation, and purification processes, nuclear waste reprocessing, and other related hydrometallurgical processes.[32,33] However, rare-earth metals, especially lanthanides, possess similar properties because of the lanthanide contraction effect.[34] They may have various possible forms, and their accurate pK_a data are more difficult to obtain experimentally than other metals.[18] In this work, the pK_a value of trivalent rare-earth metal (lanthanide and yttrium) ions were systematically studied using DFT calculations based on three proposed hydrolysis reactions and four most probable simple single-core hydrated forms. Our numerical results are subsequently compared with those from DFRT's MEP and NAO predictions. The prediction of their main existence forms at different pH values is ensued based on the results from our calculated pK_a values. This work should provide helpful insights and guidelines for the further study of the acidity for these and other aqueous rare-earth metal ions.

2. THEORETICAL MODEL

Numerous computation models of metal ion−water complexes suggest that the outer sphere water molecules have a minor impact on the ionic center through hydrogen bonding with coordinated water molecules,[25] but the hydrogen bond is generally extensive among liquid water molecules.[24,35,36] Furthermore, rare-earth ions have similar radii and coordination properties; therefore, the differences among the outer spheres of these ions are negligible. Consequently, only water molecules in the first coordination sphere are considered in this work. According to the literature, lanthanide ions generally coordinate with eight or nine water molecules.[16,37,38] The model with nine coordinated water molecules is most favorable in terms of energy, based on the computational level in this study (see the Supporting Information (SI) for details), so the nine-water coordinated model was adopted in the present work. Multicore ions are not generally present except the precipitation process, and thus, we only considered single-core metal ions for simplicity.[14,39,40] Four hydrated forms with different charges on the complex, formed by proton dissociation from the coordinated waters, namely, $[Ln(H_2O)_9]^{3+}$, $[Ln(H_2O)_8(OH)]^{2+}$, $[Ln(H_2O)_7(OH)_2]^{+}$, and $[Ln(H_2O)_6(OH)_3]$, were chosen to represent all possible forms.[25,41−43] The lowest energy geometry structure of these four species had been verified by molecular dynamics simulations as described in SI. Six structures were randomly selected from the dynamic trajectory except for the lowest and highest points as the new initiating structures to verity the geometries applied to pK_a calculation. With the gadolinium hydrate, the largest Gibbs energy differences are 0.5776, 2.1582, 0.9609, and 2.1083 kJ/mol for $[Gd(H_2O)_9]^{3+}$, $[Gd(H_2O)_8(OH)_1]^{2+}$, $[Gd(H_2O)_7(OH)_2]^{+}$, and $[Gd(H_2O)_6(OH)_3]$, respectively, and their standard deviations are less than 0.0004 kcal/mol. These results indicated that the current geometries are suitable to represent the four proposed species. The three hydrolysis reactions can be constructed as

$$[Ln(H_2O)_9]_{(aq)}^{3+} \rightarrow [Ln(H_2O)_8(OH)]_{(aq)}^{2+} + H_{(aq)}^{+}, \quad \Delta G_1 = -RTK_{a1} \tag{1}$$

$$[Ln(H_2O)_8(OH)]_{(aq)}^{2+} \rightarrow [Ln(H_2O)_7(OH)_2]_{(aq)}^{+} + H_{(aq)}^{+}, \quad \Delta G_2 = -RTK_{a2} \tag{2}$$

$$[Ln(H_2O)_7(OH)_2]_{(aq)}^{+} \rightarrow [Ln(H_2O)_6(OH)_3]_{(aq)} + H_{(aq)}^{+}, \quad \Delta G_3 = -RTK_{a3} \tag{3}$$

where ΔG_n and K_n (n = 1, 2, 3) are the Gibbs free energy and equilibrium constant, respectively. Ln represents lanthanide and yttric ions. Scandium was not included because it differs significantly from the other rare-earth elements. The water-coordinated model reported in the literature provided reliable energy values and geometries, but the proton hydration energy $\Delta G_{H^+}^{aq}$ is inaccurate.[44] Because of this, the experimental value $\Delta G_{H^+}^{aq}$ = −264.61 kcal/mol was used to calculate ΔG_n to obtain more accurate pK_a values.[22,45,46]

DOI: 10.1021/acs.jpca.7b12074
J. Phys. Chem. A 2018, 122, 700−707

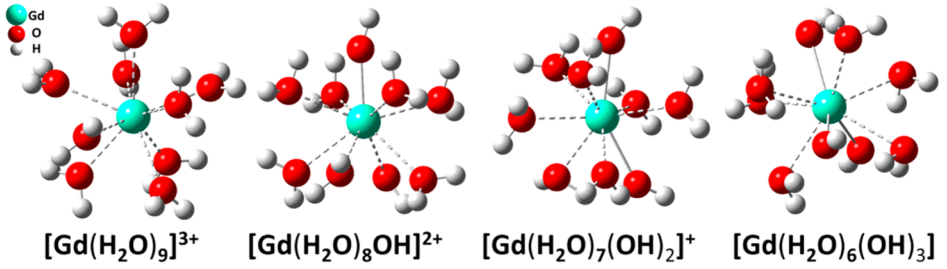

Figure 1. Four proposed metal species geometries exist in aqueous phase, exampled with Gd(III) complexes here. The other 15 element complex geometries are very similar and collected in SI.

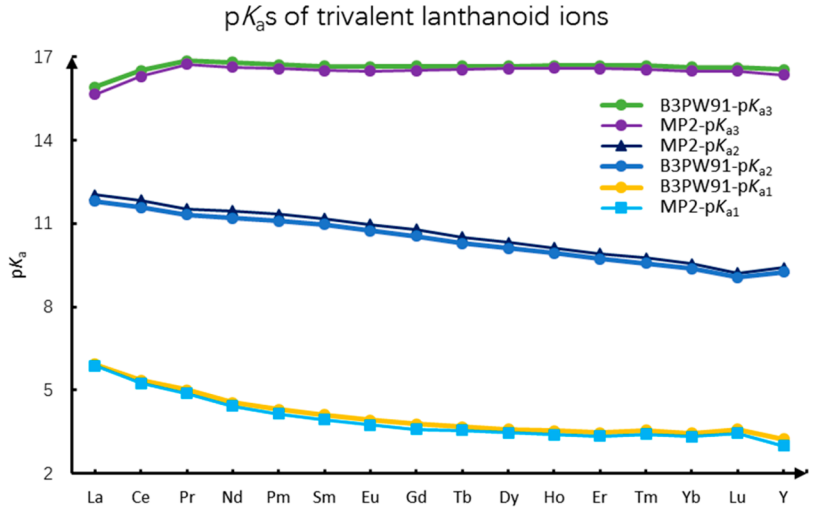

Figure 2. Computational pK_a values of lanthanide ions and yttrium. Exampled by CPCM with B3PW91 and MP2. See SI for others.

3. COMPUTATIONAL DETAILS

All geometries were fully optimized without any constraints at the B3PW91 theory level in vacuum.[47] The standard Pople basis set 6-311++G(d,p) was used for H and O atoms.[48] Metal−ligand interactions are mainly ionic, and previous studies have shown that 4f electrons take little part in coordination.[49] Therefore, we used the low-spin state and the large-core relativistic effective core potential with 4f electrons included in the core, developed by Dolg et al., namely, ECP(46+f^n)MWB for lanthanide ions and ECP28MWB for yttric ions.[50] A vibrational frequency analysis was performed for each structure to determine whether it was a minimum point (no imaginary frequency). The conformation with the lowest Gibbs free energy was selected for complexes with more than one possible conformation. The effect of solvation energy was corrected using CPCM and IEFPCM through a single-point calculation at the same theory level in water.[51] The impact of basis sets of H and O atoms and solvation models have been systematically examined with gadolinium hydrate as the examples, as described and summarized in Table S4. The conclusion can be drawn, based on this verification calculation, that the 6-311++G(d,p) are adequately accurate for both O and H elements, and the series of PCM (Polarized Continuum Model) is useful a solvation model for the pK_a calculation here. A natural bond orbital (NBO)[52] analysis was performed using a combination of the AUG-CC-PVDZ for H and O atoms[53] and the small-core relativistic effective core potential with 4f valence electrons, developed by Dolg et al.,[54] using MP2[55] or B3PW91, to understand the patterns shown in the acidity of rare-earth elements and to compute MEP and NAO quantities for the acidic oxygen and the dissociating proton. All calculations were performed using the Gaussian09, Revision D.01 package.[56]

4. RESULTS AND DISCUSSION

4.1. Optimized Structures. The previous multiple repeatedly optimized with different initiating geometries as the initial structure of $[Ln(H_2O)_9]^{3+}$ to optimize, and then a hydrogen atom in the longest O−H bond was removed to yield $[Ln(H_2O)_8(OH)]^{2+}$. Similarly, $[Ln(H_2O)_7(OH)_2]^{+}$ and $[Ln(H_2O)_6(OH)_3]$ structures were obtained subsequently. The optimized structure of these four species, using gadolinic complexes as an example, is shown in Figure 1 (see the SI for detailed structural information). $[Ln(H_2O)_9]^{3+}$ with three positive charges has approximately C_3 symmetry, with the standard deviation (SD) for the Ln−H_2O bond length ranging from 0.001 to 0.03 Å for each element. The SD value increases from La(III) to Lu(III) because of increased repulsion between the ligand water molecules as a result of the decreasing ionic radius along this sequence. In addition, the arithmetic average of the Ln−H_2O distance for each ion ranges from 2.4336 to 2.6193 Å, and this distance decreases along the atomic number sequence. These results are in good agreement with the effect of classical lanthanide contraction and ionic aqueous radius data reported by Angelo et al.[57] The Y(III) structural parameters are between those of Er(III) and Tm(III). The removal of one proton from $[Ln(H_2O)_9]^{3+}$ led to $[Ln(H_2O)_8(OH)]^{2+}$ with two positive charges and no symmetry. The Ln−OH distance of the latter structure is smaller than its Ln−H_2O distance, as expected, with their

DOI: 10.1021/acs.jpca.7b12074
J. Phys. Chem. A 2018, 122, 700−707

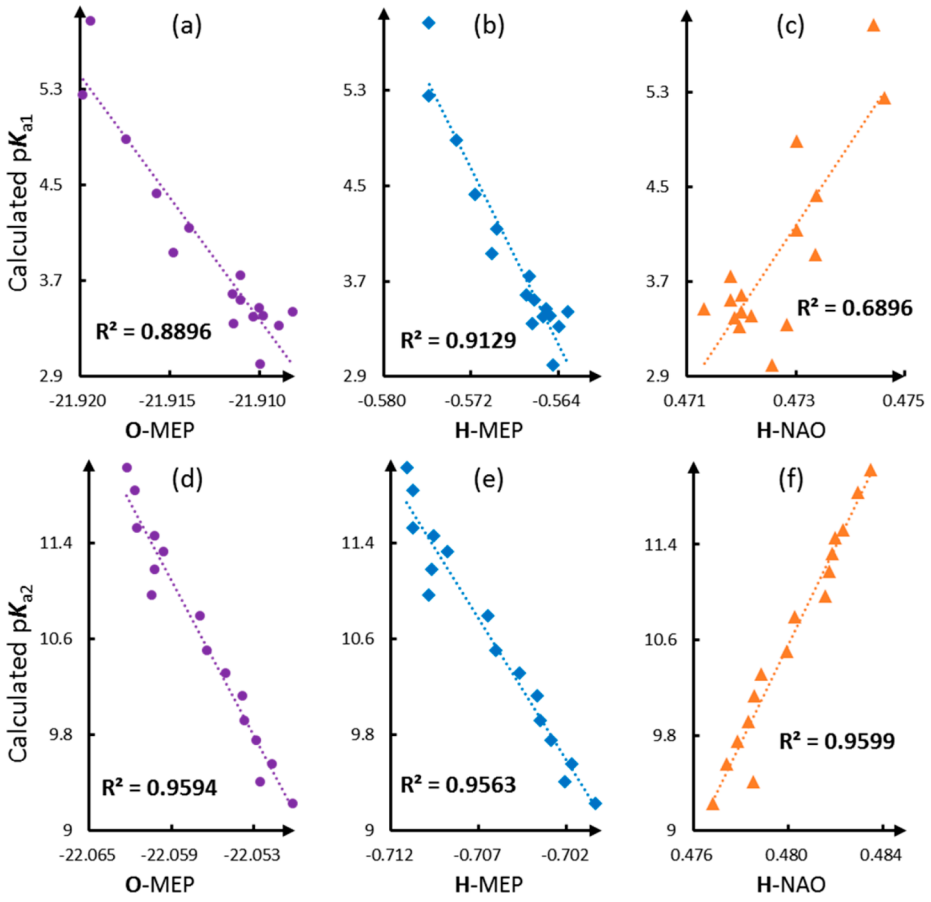

Figure 3. Approximate linear relationship between calculated pK_as and quantum descriptors. H represents the dissociation hydrogen atom, and O is its connection oxygen atom in corresponding complexes. (a–c) Linearity of pK_{a1} versus O-MEP, H-MEP, and H-NAO, respectively. (d–f) Linearity of pK_{a2} versus O-MEP, H-MEP, and H-NAO, respectively. The pK_{a3} is linear with any quantum descriptors, and the O-NAO is linear with pK_{a1} and pK_{a2}, but Lu(III) and Y(III) are singular. All numerical values are listed in SI.

distances between 2.0974–2.2097 and 2.4666–2.6605 Å, respectively. The longer Ln–H_2O bond compared to that of the species with three charges indicates that loss of a positive charge should have decreased its coordination capability. This tendency is confirmed by the data for the hydrolysis intermediates $[Ln(H_2O)_7(OH)_2]^+$ and $[Ln(H_2O)_6(OH)_3]$, and their average Ln–H_2O distances between 2.4766–2.6597 and 2.5265–2.6676 Å, respectively. The Ln–OH distance increases after proton dissociation are from 2.1012–2.2097 Å for $[Ln(H_2O)_8(OH)]^{2+}$, to 2.2148–2.3725 Å for $[Ln(H_2O)_7(OH)_2]^+$, and to 2.2500–2.4226 Å for $[Ln(H_2O)_6(OH)_3]$. These results agree well with the experimental data from spectroscopy and crystallography.[16]

4.2. Gibbs Free Energy of Hydrolysis Reaction and Ionic pK_a. The Gibbs free energies, ΔG, of the above three hydrolysis reactions can be calculated by

$$\begin{cases} \Delta G_1 = G_{[Ln(H_2O)_8(OH)]_{(aq)}{}^{2+}} - G_{[Ln(H_2O)_9]_{(aq)}{}^{3+}} + \Delta G_{H^+}{}^{aq} \\ \Delta G_2 = G_{[Ln(H_2O)_7(OH)_2]_{(aq)}{}^{+}} - G_{[Ln(H_2O)_8(OH)]_{(aq)}{}^{2+}} + \Delta G_{H^+}{}^{aq} \\ \Delta G_3 = G_{[Ln(H_2O)_6(OH)_3]_{(aq)}} - G_{[Ln(H_2O)_7(OH)_2]_{(aq)}{}^{+}} + \Delta G_{H^+}{}^{aq} \end{cases} \quad (4)$$

with their respective pK_a values obtained using the following equations:

$$\begin{cases} pK_{a1} = \dfrac{\Delta G_1}{RT \ln 10} \\ pK_{a2} = \dfrac{\Delta G_2}{RT \ln 10} \\ pK_{a3} = \dfrac{\Delta G_3}{RT \ln 10} \end{cases} \quad (5)$$

To model the solvent effect, we employed CPCM and IEFPCM, but our results show that there is little difference, less than 0.05 logarithmic units, between these two implicit solvation models. Figure 2 shows that the pK_{a2} values obtained using B3PW91 are a little smaller than those obtained using MP2, but for pK_{a1} and pK_{a3} values, the trends are opposite, with the differences less than 0.15 logarithmic units, suggesting that the differences in pK_a results using different solvation models and density functional methods are negligible. These differences become ever smaller with the increase of the atomic number of the rare-earth metal. Several pK_a values from different reports were collected in Table S6 as a comparison.

Also shown in Figure 2 is the fact that all pK_a values are positive, indicating that ΔG values obtained from eq 4 are positive for the three hydrolysis reactions. The pK_{a3} values are larger than 15.5, which do not agree with the experimental results from aqueous chemistry. Equation 3 is therefore not a reasonable representation of the hydrolysis process since it omits important factors such as aggregation.[58−60] This process

DOI: 10.1021/acs.jpca.7b12074
J. Phys. Chem. A 2018, 122, 700−707

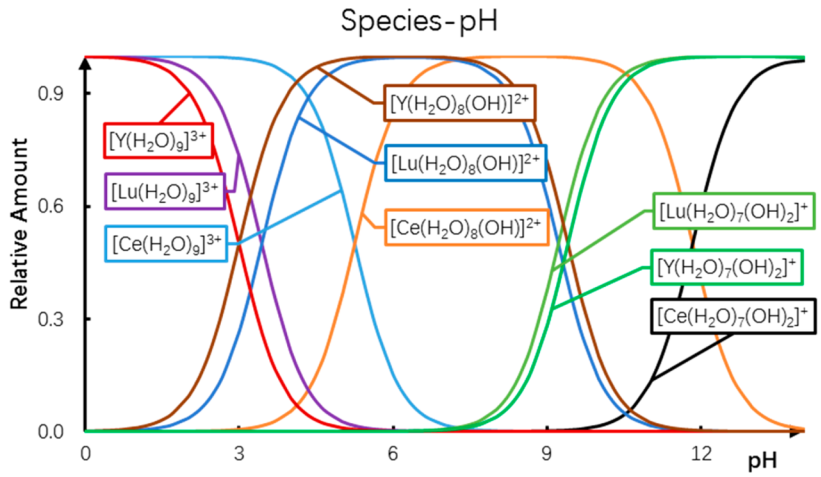

Figure 4. Estimated main ionic form at different pH based on pK_a. Ce(III), Lu(III), and Y(III) as examples; for the computation method, see SI.

of aggregation has been widely reported in the literature but will not be discussed in this work. The pK_{a1} and pK_{a2} values both decrease with an increased atomic number, showing that heavy rare-earth ions are stronger acids and can be more easily hydrolyzed than light ones. This result agrees well with previously reported experimental trends in the hydrolysis of rare-earth ions.[58−61] Additionally, Figure 2 shows that the pK_{a1} and pK_{a2} values of Y(III) are within the same range as heavy rare-earth ions. This is consistent with the usual practice and the belief that Y(III) can be regarded as a heavy rare-earth element in the extraction process, although it has a lower density than lanthanum and in different period of lanthanide series in the periodic table. The ranges of pK_{a1} and pK_{a2} values for rare-earth trivalent ions are 3.00−5.87 and 9.06−11.80, respectively, and these pK_{a1} values are close to the extraction pH value for extractants such as Cyanex272 and P227.[62] The differences of pK_{a1} values between adjacent elements are large for light rare-earth elements and become smaller for heavy ones. This trend is in good agreement with the observation that light rare-earth metal separation is easier and heavy rare-earth metal separation is more troublesome, as represented in the tetrad effect.[63] It is worth noting that the differences between adjacent elements for heavy elements are larger for pK_{a2} values than for pK_{a1} values. In addition, the yttrium possesses different properties from the lanthanide ions in pK_{a1} and pK_{a2}, this acidic property may be also used to separate the yttrium with the lanthanide ions. The separation of heavy rare-earth metal ions might therefore be more efficient if the extraction operating pH was set close to their pK_{a2} value using appropriate extractants and regents.

4.3. Understanding pK_a Values Using Quantum Descriptors. According to the findings by Liu and co-workers, there should exist strong linear correlations between pK_a values and the MEP or NAO descriptors.[3,4,22,28−30] NBO analysis was performed as described above to apply this theory to examine our systems and deepen our understanding about the factors governing the pK_a value at electronic and orbital levels. Our results are shown in Figure 3. These results are in excellent agreement with Liu's results for organic molecules and transition metal systems. Strong linear relationships were observed for O-MEP, O-NAO, H-MEP, and H-NAO with pK_{a1} or pK_{a2} values. These results confirm that the proton dissociation ability of a Brφnsted acid can be accurately measured by the changes in the MEP and NAO energies.[28−30] Rare-earth and other main-group or transition metals have the same coordinating properties, and the 4f orbital has little effect on the ligand coordination process.

4.4. Prediction of Main Forms of Metal Ions at Different pH Values. Trivalent rare-earth ionic complexes are similar to weak polyprotic acids with stepwise dissociation; therefore, their forms of existence at different pH values can be estimated and predicted by their pK_a value. All the ions have similar hydrolysis properties as shown in Figure 4, using Ce(III), Lu(III), and Y(III) as illustrative examples. The curves for $[Ln(H_2O)_6(OH)_3]$ are not included because the magnitude of pK_{a3} values is too large. Figure 4 shows that $[Ln(H_2O)_9]^{3+}$ is the main form in aqueous solution at the low pH value, and heavy rare-earth ions can be hydrolyzed at lower pH values by light rare-earth ions. $[Ln(H_2O)_8(OH)]^{2+}$ species exist mainly in the medium range of pH values but depend on the relative difference between their pK_{a1} and pK_{a2} values. It is clear that $[Y(H_2O)_8(OH)]^{2+}$ has a wider pH range than $[Lu(H_2O)_8(OH)]^{2+}$. $[Ln(H_2O)_7(OH)_2]^{+}$ is favored in high pH values. $[Ln(H_2O)_8(OH)]^{2+}$ should have a sufficiently broad range for titration. Examples of simulated titration curves are shown in SI.

4.5. Implication in Extracting Lanthanide Species. As shown in Figure 2, the range of pK_{a1} values for trivalent rare-earth ions is from 3.00 to 5.87. These values are close to the operating pH values for extraction,[11,64,65] but their main existing species is different at lower and higher pH ranges of pK_{a1} values, as shown as Figure 4. The pK_{a1} value and main existence species therefore play important roles in the extraction properties of rare-earth cations. For example, naphthenic acid and CA-12 are common extractants for the separation of yttrium from lanthanides. CA-12 is more efficient for extraction of light rare-earth ions, but less efficient for the extraction of heavy rare-earth ions. The opposite is true for naphthenic acid.[11,64,66,67] It is difficult to explain these differences based only on extractant pK_a values. Based on our results in Figure 4, however, we can see that if the ionic pK_a value is considered, the most extracted forms are $[Ln(H_2O)_8(OH)]^{2+}$ and $[Ln(H_2O)_9]^{3+}$ for heavy and light rare-earth ions, respectively, at the operating pH value range of 4 to 5. In coordination with the extractant and hydrated metal ions, the hydroxyl group in $[Ln(H_2O)_8(OH)]^{2+}$ may experience significantly strong repulsion with the ether oxygen in CA-12, leading to the lower extractability of heavy rare-earth

DOI: 10.1021/acs.jpca.7b12074
J. Phys. Chem. A 2018, 122, 700−707

ions, and thus little separation of Y(III) from other ions. In contrast, when naphthenic acid is used as the extractant, which is an ordinary carboxylic acid with a different carbon chain, the repulsive interaction mentioned above between the hydroxyl group of $[Ln(H_2O)_8(OH)]^{2+}$ and the extractant should be similar for both yttrium and lanthanides, and thus yield desirable results as we expected.

5. CONCLUSION

Several conclusions can be drawn from the results presented and discussed above. At first, our results show that a simplified first-order approximation for mononuclear metal−water complexes should be suitable for studying the acidity of rare-earth metal ions, and no complicated model systems are needed. Second, the stepwise pK_a value calculated from hydrolysis reactions can be used to predict the main forms of metal ions at different pH values in aqueous environment. Third, the acidity of rare-earth metal−water complexes in aqueous solution can be adequately described by quantum descriptors such as molecular electrostatic potential or natural atomic orbital energy of the acidic oxygen or dissociated proton, same as main-group or transition-metal cations and organic acids. Finally, the main ionic forms obtained using predicted pK_a values can be simulated, and they will have tremendous implications for the efficient extraction and separation of rare-earth metal ions in hydrometallurgy. These applications will be further explored in our future investigations, whose results will be presented elsewhere.

■ ASSOCIATED CONTENT

Supporting Information

The Supporting Information is available free of charge on the ACS Publications website at DOI: 10.1021/acs.jpca.7b12074.

All optimized geometry structures of metal−water complex and their hydrolysis product, reaction energies from $[Ln(H_2O)_8]^{3+}$ to $[Ln(H_2O)_9]^{3+}$, calculated pK_as at several conditions, dynamic results, tests of basis sets and solution models, value of MEP and NAO for various metal-complexes and their correlation coefficients with pK_as, the computation method of main ionic form, simulated titration curve, entire Gaussian reference, and comparison of pK_a values from different references (PDF)

■ AUTHOR INFORMATION

Corresponding Authors

*E-mail: jchxiao@sioc.ac.cn.
*E-mail: smxu@tsinghua.edu.cn.
*E-mail: shubin@email.unc.edu.

ORCID

Donghai Yu: 0000-0002-3119-7999
Ji-Chang Xiao: 0000-0001-8881-1796
Shengming Xu: 0000-0002-6765-9251
Shubin Liu: 0000-0001-9331-0427

Notes

The authors declare no competing financial interest.

■ ACKNOWLEDGMENTS

The authors thank National Basic Research Program of China (2015CB931903), the National Natural Science Foundation (21421002, 21472222, 21502214, 21672242), the Chinese Academy of Sciences (XDA02020105, XDA02020106), Key Research Program of Frontier Sciences (CAS) (QYZDJ-SSW-SLH049), and State Key Laboratory of Nickel and Cobalt Resources Comprehensive Utilization (jinkeye 2017-05) for financial support. D.H.Y. and C.Y.R. acknowledge supports from Hunan Provincial Natural Science Foundation of China (Grant No. 2017JJ3201) and Scientific Research Fund of Hunan Provincial Education Department (Grant No. 17C0949). Computing resources were provided by the National Supercomputing Center of China in Shenzhen.

■ REFERENCES

(1) Thapa, B.; Schlegel, H. B. DFT Calculation of pK_a's of Thiols in Aqueous Solution Using Explicit Water Molecules and Polarizable Continuum Model. *J. Phys. Chem. A* **2016**, *120*, 5726−5735.
(2) Seybold, P. G.; Shields, G. C. Computational estimation of pK_a values. *WIREs: Comput. Mol. Sci.* **2015**, *5*, 290−297.
(3) Huang, Y.; Liu, L. H.; Liu, W. H.; Liu, S. H.; Liu, S. B. Modeling Molecular Acidity with Electronic Properties and Hammett Constants for Substituted Benzoic Acids. *J. Phys. Chem. A* **2011**, *115*, 14697−14707.
(4) Burger, S. K.; Liu, S. B.; Ayers, P. W. Practical Calculation of Molecular Acidity with the Aid of a Reference Molecule. *J. Phys. Chem. A* **2011**, *115*, 1293−1304.
(5) Manallack, D. T.; Prankerd, R. J.; Yuriev, E.; Oprea, T. I.; Chalmers, D. K. The significance of acid/base properties in drug discovery. *Chem. Soc. Rev.* **2013**, *42*, 485−496.
(6) Takaoka, T.; Sakashita, N.; Saito, K.; Ishikita, H. pK_a of a Proton-Conducting Water Chain in Photosystem II. *J. Phys. Chem. Lett.* **2016**, *7*, 1925−1932.
(7) Meyer, T.; Knapp, E.-W. pK_a Values in Proteins Determined by Electrostatics Applied to Molecular Dynamics Trajectories. *J. Chem. Theory Comput.* **2015**, *11*, 2827−2840.
(8) Chen, X.; Stace, A. J. A gas phase perspective on the Lewis acidity of metal ions in aqueous solution. *Chem. Commun.* **2012**, *48*, 10292−10294.
(9) Galstyan, G.; Knapp, E.-W. Computing pK_a values of hexa-aqua transition metal complexes. *J. Comput. Chem.* **2015**, *36*, 69−78.
(10) Ivanov, A. S.; Bryantsev, V. S. A Computational Approach to Predicting Ligand Selectivity for the Size-Based Separation of Trivalent Lanthanides. *Eur. J. Inorg. Chem.* **2016**, *2016*, 3474−3479.
(11) Li, D. A review on yttrium solvent extraction chemistry and separation process. *J. Rare Earths* **2017**, *35*, 107−119.
(12) Sillen, L. G.; Martell, A. E. *Stability Constants of Metal-Ion Complexes*; The Chemical Society: London U.K., 1964.
(13) Sisley, M. J.; Jordan, R. B. First Hydrolysis Constants of Hexaaquacobalt(III) and -manganese(III): Longstanding Issues Resolved. *Inorg. Chem.* **2006**, *45*, 10758−10763.
(14) Jackson, V. E.; Felmy, A. R.; Dixon, D. A. Prediction of the pK_a's of Aqueous Metal Ion + 2 Complexes. *J. Phys. Chem. A* **2015**, *119*, 2926−2939.
(15) Kuter, D.; Streltsov, V.; Davydova, N.; Venter, G. A.; Naidoo, K. J.; Egan, T. J. Molecular Structures and Solvation of Free Monomeric and Dimeric Ferriheme in Aqueous Solution: Insights from Molecular Dynamics Simulations and Extended X-ray Absorption Fine Structure Spectroscopy. *Inorg. Chem.* **2014**, *53*, 10811−10824.
(16) Persson, I.; D'angelo, P.; De Panfilis, S.; Sandström, M.; Eriksson, L. Hydration of Lanthanoid(III) Ions in Aqueous Solution and Crystalline Hydrates Studied by EXAFS Spectroscopy and Crystallography: The Myth of the "Gadolinium Break. *Chem. - Eur. J.* **2008**, *14*, 3056−3066.
(17) Hawkes, S. J. All Positive Ions Give Acid Solutions in Water. *J. Chem. Educ.* **1996**, *73*, 516−517.
(18) Burgess, J. *Metal Ions in Solution*; Ellis Horwood Ltd: Hempstead Herts, U.K., 1978.
(19) Rustad, J. R.; Dixon, D. A.; Felmy, A. R. Intrinsic acidity of aluminum, chromium (III) and iron (III) μ_3-hydroxo functional

DOI: 10.1021/acs.jpca.7b12074
J. Phys. Chem. A 2018, 122, 700−707

groups from ab initio electronic structure calculations. *Geochim. Cosmochim. Acta* **2000**, *64*, 1675−1680.
(20) Sillén, L. G.; et al. High-speed Computers as Supplement to Graphical Methods. I. Functional Behavior of the Error Square Sum. *Acta Chem. Scand.* **1962**, *16*, 159−172.
(21) Rustad, J. R.; Dixon, D. A.; Rosso, K. M.; Felmy, A. R. Trivalent Ion Hydrolysis Reactions: A Linear Free-Energy Relationship Based on Density Functional Electronic Structure Calculations. *J. Am. Chem. Soc.* **1999**, *121*, 3234−3235.
(22) Liu, S. B.; Schauer, C. K.; Pedersen, L. G. Molecular acidity: A quantitative conceptual density functional theory description. *J. Chem. Phys.* **2009**, *131*, 164107−164114.
(23) Sweeney, A. F.; Armentrout, P. B. Guided Ion Beam Studies of the Collision-Induced Dissociation of $CuOH^+(H_2O)_n$ (n = 1−4): Comprehensive Thermodynamic Data for Copper Ion Hydration. *J. Phys. Chem. A* **2014**, *118*, 10210−10222.
(24) Bogatko, S.; Cauët, E.; Geerlings, P. Influence of F− Coordination on Al^{3+} Hydrolysis Reactions from Density Functional Theory Calculations. *J. Phys. Chem. C* **2011**, *115*, 6910−6921.
(25) Wander, M. C. F.; Rustad, J. R.; Casey, W. H. Influence of Explicit Hydration Waters in Calculating the Hydrolysis Constants for Geochemically Relevant Metals. *J. Phys. Chem. A* **2010**, *114*, 1917−1925.
(26) Thapa, B.; Schlegel, H. B. Density Functional Theory Calculation of pK_a's of Thiols in Aqueous Solution Using Explicit Water Molecules and the Polarizable Continuum Model. *J. Phys. Chem. A* **2016**, *120*, 5726−5735.
(27) Liu, S. B.; Pedersen, L. G. Estimation of Molecular Acidity via Electrostatic Potential at the Nucleus and Valence Natural Atomic Orbitals. *J. Phys. Chem. A* **2009**, *113*, 3648−3655.
(28) Zhao, D. B.; Rong, C. Y.; Yin, D. L.; Liu, S. B. Molecular Acidity of Building Blocks of Biological Systems: A Density Functional Reactivity Theory Study. *J. Theor. Comput. Chem.* **2013**, *12*, 1350034−1350045.
(29) Huang, Y.; Zhong, A. G.; Liu, S. B. Predicting pK_a Values for Singly and Multiply Substituted Benzoic Acids with Density Functional Reactivity Theory. *J. Nat. Sci. HNNU* **2011**, *34*, 52−55.
(30) Huang, Y.; Liu, L. B.; Liu, S. B. Towards understanding proton affinity and gas-phase basicity with density functional reactivity theory. *Chem. Phys. Lett.* **2012**, *527*, 73−78.
(31) Lim, X. Chemistry: Degrees of separation. *Nature* **2015**, *520*, 426−427.
(32) Jha, M. K.; Kumari, A.; Panda, R.; Rajesh Kumar, J.; Yoo, K.; Lee, J. Y. Review on hydrometallurgical recovery of rare earth metals. *Hydrometallurgy* **2016**, *165* (Part 1), 2−26.
(33) Cotton, S. A. Scandium, yttrium, the lanthanides. *Annu. Rep. Prog. Chem., Sect. A: Inorg. Chem.* **2012**, *108*, 251−260.
(34) Ferru, G.; Reinhart, B.; Bera, M. K.; Olvera De La Cruz, M.; Qiao, B.; Ellis, R. J. The Lanthanide Contraction beyond Coordination Chemistry. *Chem. - Eur. J.* **2016**, *22*, 6899−6904.
(35) Radoń, M.; Gąssowska, K.; Szklarzewicz, J.; Broclawik, E. Spin-State Energetics of Fe(III) and Ru(III) Aqua Complexes: Accurate ab Initio Calculations and Evidence for Huge Solvation Effects. *J. Chem. Theory Comput.* **2016**, *12*, 1592−1605.
(36) Tirler, A. O.; Passler, P. P.; Rode, B. M. The lanthanoid hydration properties beyond the 'Gadolinium Break': Dysprosium (III) and holmium (III), an ab initio quantum mechanical molecular dynamics study. *Chem. Phys. Lett.* **2015**, *635*, 120−126.
(37) D'angelo, P.; Spezia, R. Hydration of Lanthanoids(III) and Actinoids(III): An Experimental/Theoretical Saga. *Chem. - Eur. J.* **2012**, *18*, 11162−11178.
(38) Zhang, J.; Heinz, N.; Dolg, M. Understanding Lanthanoid(III) Hydration Structure and Kinetics by Insights from Energies and Wave functions. *Inorg. Chem.* **2014**, *53*, 7700−7708.
(39) Yang, W.; Qian, Z.; Miao, Q.; Wang, Y.; Bi, S. Density functional theory study of the aluminium(iii) hydrolysis in aqueous solution. *Phys. Chem. Chem. Phys.* **2009**, *11*, 2396−2401.
(40) Baes, C. F.; Mesmer, R. E. *The Hydrolysis of Cations*; John Wiley & Sons Inc: New York, 1976.
(41) De Abreu, H. A.; Guimarães, L.; Duarte, H. A. Density-Functional Theory Study of Iron(III) Hydrolysis in Aqueous Solution. *J. Phys. Chem. A* **2006**, *110*, 7713−7718.
(42) Liu, X.; Lu, X.; Meijer, E. J.; Wang, R.; Zhou, H. Acid dissociation mechanisms of $Si(OH)_4$ and $Al(H_2O)_6^{3+}$ in aqueous solution. *Geochim. Cosmochim. Acta* **2010**, *74*, 510−516.
(43) Gilson, R.; Durrant, M. C. Estimation of the pK_a values of water ligands in transition metal complexes using density functional theory with polarized continuum model solvent corrections. *Dalton Trans.* **2009**, 10223−10230.
(44) Shi, R.; Huang, X.; Su, Y.; Lu, H.-G.; Li, S.-D.; Tang, L.; Zhao, J. Which Density Functional Should Be Used to Describe Protonated Water Clusters? *J. Phys. Chem. A* **2017**, *121*, 3117−3127.
(45) Palascak, M. W.; Shields, G. C. Accurate Experimental Values for the Free Energies of Hydration of H^+, OH^-, and H_3O^+. *J. Phys. Chem. A* **2004**, *108*, 3692−3694.
(46) Camaioni, D. M.; Schwerdtfeger, C. A. Comment on "Accurate Experimental Values for the Free Energies of Hydration of H^+, OH^-, and H_3O^+. *J. Phys. Chem. A* **2005**, *109*, 10795−10797.
(47) Perdew, J. P.; Chevary, J. A.; Vosko, S. H.; Jackson, K. A.; Pederson, M. R.; Singh, D. J.; Fiolhais, C. Atoms, molecules, solids, and surfaces: Applications of the generalized gradient approximation for exchange and correlation. *Phys. Rev. B: Condens. Matter Mater. Phys.* **1992**, *46*, 6671−6687.
(48) Rassolov, V. A.; Ratner, M. A.; Pople, J. A.; Redfern, P. C.; Curtiss, L. A. 6-31G* basis set for third-row atoms. *J. Comput. Chem.* **2001**, *22*, 976−984.
(49) Du, R.; Yu, D.; An, H.; Zhang, S.; Lu, R.; Zhao, G.; Xiao, J.-C. *α,β*-Substituent effect of dialkylphosphinic acids on lanthanide extraction. *RSC Adv.* **2016**, *6*, 56004−56008.
(50) Dolg, M. Segmented Contracted Douglas−Kroll−Hess Adapted Basis Sets for Lanthanides. *J. Chem. Theory Comput.* **2011**, *7*, 3131−3142.
(51) Cramer, C. J.; Truhlar, D. G. Implicit Solvation Models: Equilibria, Structure, Spectra, and Dynamics. *Chem. Rev.* **1999**, *99*, 2161−2200.
(52) Reed, A. E.; Curtiss, L. A.; Weinhold, F. Intermolecular interactions from a natural bond orbital, donor-acceptor viewpoint. *Chem. Rev.* **1988**, *88*, 899−926.
(53) Bohmann, J. A.; Weinhold, F.; Farrar, T. C. Natural chemical shielding analysis of nuclear magnetic resonance shielding tensors from gauge-including atomic orbital calculations. *J. Chem. Phys.* **1997**, *107*, 1173−1184.
(54) Cao, X.; Dolg, M. Valence basis sets for relativistic energy-consistent small-core lanthanide pseudopotentials. *J. Chem. Phys.* **2001**, *115*, 7348−7355.
(55) Head-Gordon, M.; Head-Gordon, T. Analytic MP2 frequencies without fifth-order storage. Theory and application to bifurcated hydrogen bonds in the water hexamer. *Chem. Phys. Lett.* **1994**, *220*, 122−128.
(56) Frisch, M., et al. *Gaussian 09*, revision D.01; Gaussian, Inc.: Wallingford, CT, 2013.
(57) D'angelo, P.; Zitolo, A.; Migliorati, V.; Chillemi, G.; Duvail, M.; Vitorge, P.; Abadie, S.; Spezia, R. Revised Ionic Radii of Lanthanoid-(III) Ions in Aqueous Solution. *Inorg. Chem.* **2011**, *50*, 4572−4579.
(58) Luo, Q.-H.; Shen, M.-C.; Ding, Y.; Chen, Z.-D. Studies on hydrolytic polymenrization of rare earth ions II. hydrolytic polymenrization of Sm^{3+} ion. *Acta. Chim. Sin.* **1983**, *41*, 1115−1120.
(59) Luo, Q.; Ding, Y.; Shen, M. Studies on hydrolytic polymenrization of rare earth ions IV. hydrolytic polymenrization of Yb^{3+} ion. *J. Chin. Soc. Rare. Earth.* **1988**, *6*, 73−74.
(60) Luo, Q.; Ding, Y.; Shen, M. Studies on hydrolytic polymenrization of rare earth ions IV. hydrolytic polymenrization of Eu^{3+} and Gd^{3+} ion. *Chem. J. Chin. Univ.* **1985**, *6*, 201−205.
(61) Cigala, R. M.; De Stefano, C.; Irto, A.; Milea, D.; Sammartano, S. Thermodynamic Data for the Modeling of Lanthanoid(III) Sequestration by Reduced Glutathione in Aqueous Solution. *J. Chem. Eng. Data* **2015**, *60*, 192−201.

DOI: 10.1021/acs.jpca.7b12074
J. Phys. Chem. A 2018, 122, 700−707

(62) Yu, D.; Du, R.; Xiao, J.-C. pK_a prediction for acidic phosphorus-containing compounds using multiple linear regression with computational descriptors. *J. Comput. Chem.* **2016**, *37*, 1668−1671.
(63) Peppard, D. F.; Mason, G. W.; Lewey, S. A tetrad effect in the liquid-liquid extraction ordering of lanthanides(III). *J. Inorg. Nucl. Chem.* **1969**, *31*, 2271−2272.
(64) Wang, W.; Yang, H.; Liu, Y.; Cui, H.; Chen, J. The application of biodiesel and *sec*-octylphenoxyacetic acid (CA-12) for the yttrium separation. *Hydrometallurgy* **2011**, *109*, 47−53.
(65) Wang, W.; Yang, H.; Cui, H.; Zhang, D.; Liu, Y.; Chen, J. Application of Bifunctional Ionic Liquid Extractants [A336][CA-12] and [A336][CA-100] to the Lanthanum Extraction and Separation from Rare Earths in the Chloride Medium. *Ind. Eng. Chem. Res.* **2011**, *50*, 7534−7541.
(66) Liu, K.; Wang, Z.; Tang, X.; Lu, S. Extraction of yttrium using naphthenic acid with different acid numbers. *Sep. Sci. Technol.* **2016**, *51*, 2804−2814.
(67) Wang, Y.; Liao, W.; Li, D. A solvent extraction process with mixture of CA12 and Cyanex272 for the preparation of high purity yttrium oxide from rare earth ores. *Sep. Purif. Technol.* **2011**, *82*, 197−201.

DOI: 10.1021/acs.jpca.7b12074
J. Phys. Chem. A 2018, 122, 700−707